3354–3361 *Nucleic Acids Research, 1997, Vol. 25, No. 16*

Structure of the hydrogen bonding complex of O^6-methylguanine with cytosine and thymine during DNA replication

Thomas E. Spratt* and Douglas E. Levy

American Health Foundation, Division of Pathology and Toxicology, 1 Dana Road, Valhalla, NY 10595, USA

Received March 10, 1997; Revised and Accepted June 26, 1997

ABSTRACT

During DNA replication, mutations occur when an incorrect dNTP is incorporated opposite a carcinogen-modified nucleotide. We have probed the structures of the interaction between O^6-methylguanine (O^6mG) and cytosine and thymine during replication by kinetic means in order to examine the structure during the rate determining step. The kinetics of incorporation of dCTP and dTTP opposite O^6mG and three analogs, S^6-methyl-6-thioguanine, O^6-methyl-1-deazaguanine and O^6-methylhypoxanthine, have been measured with four polymerases, the Klenow fragment of DNA polymerase I, the Klenow fragment with the proof-reading exonuclease inactivated, Taq and Tth polymerases. In the insertion of dTTP opposite O^6mG, a large decrease in V_{max}/K_m was observed only upon modification of the N1 position. This result is consistent with a Watson–Crick type configuration. For the incorporation of dCTP, the V_{max}/K_m was significantly decreased only with removal of the exocyclic amino group at the 2 position. The pH dependence of the ratio of incorporation of dCTP and dTTP was independent of pH at physiological pH. This result suggests that dCTP is incorporated via an uncharged complex such as the wobble configuration.

INTRODUCTION

Carcinogen-modified DNA leads to mutations when the DNA polymerase incorporates an incorrect dNTP opposite the lesion. The identity of the lesion can have an influence on which nucleotide is incorporated opposite it through hydrogen bonding. Loveless (1) proposed that O^6-alkylguanines can cause mutations because alkylation alters the hydrogen bonding region of guanine. Upon alkylation of the oxygen, the 1 position of guanine is changed from a hydrogen bond donor to a hydrogen bond acceptor. Consequently, specific hydrogen bonding to cytosine is destroyed and the potential exists for a favorable hydrogen bonding complex with thymine. In this manuscript we describe our investigations into the structure of the hydrogen bonding complex between O^6mG1 and dCTP and dTTP during replication using analogs of O^6mG in which the Watson–Crick hydrogen bonding sites have been altered.

Replication of normal nucleotides involves the formation of Watson–Crick base pairs between the template and the dNTP. The difference in energy between the correct and incorrect base pairs in aqueous solution is not large enough to account for the fidelity (2). The polymerase may enhance the free energy differences by reducing the entropy differences of the correct and incorrect base pairs (3). In addition, the exclusion of water from the active site of the protein can increase the difference in energy between the correct and incorrect base pairs (4). Fidelity is also controlled further along the replication pathway. After binding of the dNTP to the template, the polymerase undergoes a conformational change which can allow the polymerase to provide steric checks to determine whether the DNA has the Watson–Crick conformation. If the nascent base pair and the previous 3 bp are of the Watson–Crick configuration then phosphodiester bond formation proceeds quickly. If not, then phosphodiester bond formation is rate limiting (5).

dCTP and dTTP were found to be incorporated opposite O^6mG *in vitro* (6,7) and *in vivo* (8–12). In the *in vitro* reactions, the rate of incorporation opposite O^6mG is much less than for the natural bases and similar to the misincorporation of dTTP opposite G with the Klenow fragment (7,13). Phosphodiester bond formation is rate limiting and differences in the rate of the phosphodiester bond formation can account for the preferential incorporation of dTTP opposite O^6mG (14).

The stability of the base pair between O^6mG and dC or dT does not directly influence which nucleotide is incorporated. Based on melting studies, the O^6mG–dC complex is more stable than O^6mG–dT complex (15,16) but dTTP is incorporated opposite O^6mG more frequently than dCTP.

The structure of the complexes may explain the preference for dTTP over dCTP. Potential structures for the O^6mG–dNTP complex during replication can be obtained by examining the static structures obtained by NMR and X-ray crystallographic techniques. NMR studies of an oligodeoxynucleotide duplex have shown that the O^6mG–dT complex is in the distorted Watson–Crick configuration, as illustrated in Figure 1a. The methyl group is oriented in the *syn* configuration, pointing toward the opposite DNA stand (17,18). Molecular modeling studies have shown that the methyl group is more stable in the *syn*

* To whom correspondence should be addressed. Tel: +1 914 789 7289; Fax: +1 914 592 6317; Email: tomspratt@aol.com

configuration in the nucleoside, but the energy difference is only ~1 kcal/mol. Depending on the environment, the methyl group is able to interconvert between the *syn* and *anti* configurations (19). The more Watson–Crick-like structure illustrated in Figure 1b, with the methyl group in the *anti* configuration, has been observed in a crystal of an oligodeoxynucleotide duplex (15) as well as with protected nucleosides in $CDCl_3$ (20).

The O^6mG–dC base pair has been found to exist in three different conformations. NMR studies of a duplex have detected the wobble structure illustrated in Figure 2a (21,22). An X-ray crystallographic study of an oligodeoxynucleotide duplex with netropsin bound to the minor groove found a O^6mG–dC base pair to be a wobble structure (Fig. 2a) and a second O^6mG–dC base pair to be in a bifurcated structure with split hydrogen bonds, as illustrated in Figure 2b (23). The more Watson–Crick-like protonated structure illustrated in Figure 2c has been observed in a crystal structure (24) and with protected nucleosides in $CDCl_3$ (20). Melting studies over a pH range suggest that at low pH the O^6mG–dC structure is protonated as in Figure 2c but is neutral at physiological pH (15).

We probed the structure of the complex between the incoming dNTP and O^6mG by examining this reaction with analogs of O^6mG in which the hydrogen bonding region is chemically changed. This interaction was also examined by determining the pH dependence of the insertion of dCTP and dTTP.

MATERIALS AND METHODS

Chemicals

[^{32}P]ATP was purchased from Amersham (Arlington Heights, IL) at 6000 Ci/mmol. T4 polynucleotide kinase, Taq DNA polymerase, Tth DNA polymerase, the Klenow fragment of *Escherichia coli* DNA polymerase I and the Klenow fragment with the proof-reading exonuclease inactivated [Kf(exo$^-$)] were obtained from US Biochemicals (Cleveland, OH). The dNTPs were purchased from Pharmacia (Uppsala, Sweden) as ultrapure grade and the concentrations were checked by absorbance (25).

Synthesis of oligodeoxynucleotides

The oligonucleotides were synthesized and characterized similarly to as previously described (26,27). The oligodeoxynucleotides synthesized include the primer and the template strands of the sequences described below. The primers were synthesized in which N was either C or T. The templates were synthesized in which X was G, O^6mG, S^6mG, O^6m1DG or O^6mH. The oligodeoxynucleotides were purified by a combination of anion exchange and reverse phase HPLC (27). The purities of the oligodeoxynucleotides were determined to be >98% by PAGE with the 5′-[^{32}P]O_4-labeled oligodeoxynucleotides. The sequences were chosen to alternate the nucleotides but to keep a higher CG content, so that the template–primer complex would stay annealed at a reasonable temperature and that the primer would anneal to the template in the correct position. The concentrations of oligodeoxynucleotides were determined from the absorbance at 260 nm, using ε = 115/mM/cm for the primer and 172/mM/cm for the template (28). The primer was ^{32}P-labeled with [γ-^{32}P]ATP and T4 polynucleotide kinase. The oligomer was separated from low molecular weight impurities with a spin column (BioGel P6; Sigma, St Louis, MO) and the primer was annealed with a 10% excess of the template as described (27).

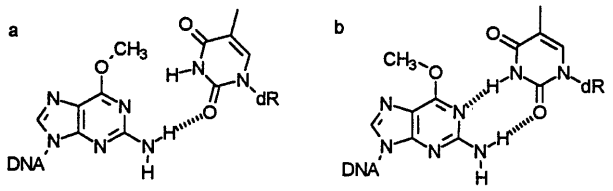

Figure 1. Possible O^6mG:T base pair configurations. (**a**) NMR solution structure (21,22); (**b**) X-ray crystal structure (15), solution structure of protected nucleosides in $CDCl_3$ (20).

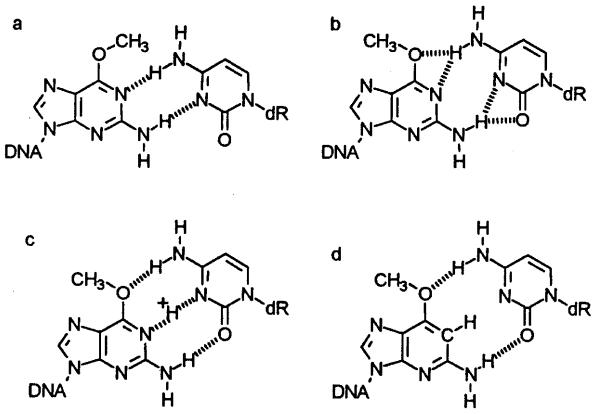

Figure 2. Possible O^6mG:C base pair configurations. (**a**) X-ray crystal structure (23), NMR solution structure (17,18); (**b**) X-ray crystal structure (23); (**c**) X-ray crystal structure (24), solution structure of protected nucleosides in $CDCl_3$ (20); (**d**) proposed base pair configuration between O^6m1DG and dC.

template: 3′-GCTGCAGCTGCAXCTAGT-5′
P 12 5′-CGACGTCGACGT-3′
P 13N 5′-CGACGTCGACGTN-3′

Reaction with DNA polymerase

The polymerase was added to a solution containing a ^{32}P-labeled oligodeoxynucleotide duplex and the buffer was adjusted to the final conditions of 100 mM buffer, 10 mM $MgCl_2$, 10 mM DTT, 200 μg/ml BSA. The reaction was initiated by addition of 3 μl dNTP in water to 3 μl DNA/enzyme solution at 37°C. The composition of the buffer during the reaction was 50 mM buffer, 5 mM $MgCl_2$, 5 mM DTT, 100 μg/ml BSA. The reactions were quenched by addition of 6 μl 100 mM EDTA in 95% formamide. The progress of the reaction was analyzed by denaturing PAGE in 20% acrylamide (19:1, acrylamide:*N*,*N*′-methylene bisacrylamide), 7 M urea in 1× TBE buffer (0.089 M Tris, 0.089 M boric acid, 0.002 M Na_2EDTA). The size of the gel was 40 × 33 × 0.4 cm and was run at 2500 V for 2–2.5 h. The radioactivity on the gel was determined with an Ambis Radioanalytic Imaging System or a BioRad GS 250 Molecular Imager.

Insertion opposite guanine, O^6mG and analogs

The incorporation of dCTP and dTTP opposite G, O^6mG, S^6mG, O^6m1DG and O^6mH was carried out using 50 mM Tris–HCl, pH 8.0, as buffer. The concentration of primer was 190 nM for reaction with the Klenow fragments and 200 nM for the reactions

with Taq and Tth DNA polymerases. The polymerase concentrations were 0.45 U/ml Kf(exo$^-$), 0.23 U/ml for Kf(exo$^+$) and 18.8 U/ml for Taq and Tth DNA polymerases. These concentrations of polymerases were employed to obtain 3–20% yield of product in 1–10 min incubations. The activity of Taq and Tth DNA polymerases are calculated at 70°C and are less active at 37°C. The concentration of dCTP and dTTP varied from 0 to 1 mM.

Extension past *O*^{6}mG–C and *O*^{6}mG–T base pairs

The extension reactions were performed as described above using primer 13C and primer 13T annealed to the template with Kf(exo$^-$) at 0.45 U/ml. The initial rate of incorporation of dGTP over a range of concentrations was determined.

pH dependency for incorporation opposite *O*^{6}mG

The pH of the buffer was adjusted by addition of HCl while the ionic strength was kept at a constant by addition of NaCl. The final buffer concentration was 50 mM buffer–HCl, 5 mM $MgCl_2$, 5 mM DTT, 100 μg/ml BSA, with an ionic strength of 65 mM. The buffers used were MES, pH 5–6.5, HEPES, pH 6.5–8.0, and TAPS, pH 8.0–9.5. Kf(exo$^-$) was incubated with buffer and DNA at 37°C for at least 10 min prior to initiation of the reaction. To measure competition between dCTP and dTTP, the DNA and polymerase were incubated with 20 μM dTTP and 120 μM dTTP.

Incorporation of 2′-deoxyuridine and 5-methyl-2′-deoxycytidine

The initial rate of incorporation of dUTP and d5mCTP opposite *O*^{6}mG was carried out as described for incorporation of dTTP and dCTP.

RESULTS AND DISCUSSION

Incorporation of dCTP and dTTP opposite analogs of *O*^{6}mG

Interactions in the hydrogen bonding region between *O*^{6}mG and dCTP and dTTP were explored using the analogs of *O*^{6}mG illustrated in Figure 3. If a site was important for the reaction then alteration of that site should decrease the rate of reaction. An assumption is that these changes are minor compared with methylation and that the DNA–polymerase complex treats the *O*^{6}mG analogs as *O*^{6}mG. Nucleotide analogs have been employed to examine internucleotide interactions (29), protein–DNA interactions (30,31) and the mechanism of DNA polymerase (32). Substitutions in *O*^{6}mG can result in a suboptimal interaction due to steric hindrance and disruption of a hydrogen bond. Sulfur is larger than oxygen and less electronegative. Thus, if a dNTP was in a hydrogen bond with the O^6 position of *O*^{6}mG then changing oxygen to sulfur would push the dNTP further away due to a steric effect and it would be bound less tightly due to a weaker hydrogen bond. Substitution of sulfur in the 6 position of guanine has been found to decrease the rate of incorporation of dCTP by 60% (33,34). The replacement of N with CH results in the loss of a hydrogen bond acceptor in *O*^{6}m1DG. Furthermore,

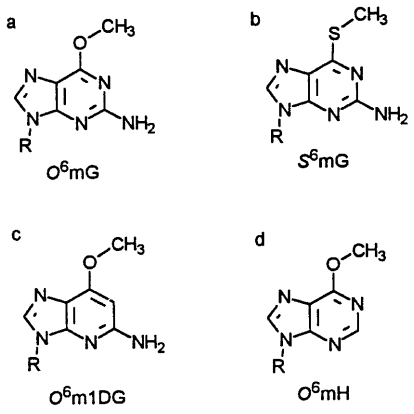

Figure 3. Analogs of *O*^{6}mG. (**a**) *O*^{6}mG; (**b**) *S*^{6}-methyl-6-thioguanine (*S*^{6}mG); (**c**) *O*^{6}-methyl-1-deazaguanine (*O*^{6}m1DG); (**d**) *O*^{6}-methylhypoxanthine (*O*^{6}mH).

the carbon-bound proton would also sterically interfere with any proton that had been in a hydrogen bond with the nitrogen. This interaction would significantly distort the *O*^{6}mG–dNTP complex. A hydrogen bond donor is removed with *O*^{6}mH. The strength of the interactions with the 2-carbonyl on the dNTP would be reduced. However, there are no steric interactions that prevent the structure of the *O*^{6}mH–dNTP complex being similar to the *O*^{6}mG–dNTP complex. In incorporation of dCTP opposite guanine, removal of the amino group reduced the rate of reaction ~10-fold (35).

The rates of replication of *O*^{6}mG and these analogs were determined for four polymerases, the Klenow fragment, Kf(exo$^-$), Taq and Tth polymerase. The kinetics of insertion of dCTP or dTTP opposite the lesion and extension past the lesion were followed by PAGE, which separates the starting material and the products. The kinetics was found to be consistent with simple Michaelis–Menten kinetics illustrated by equations **1** and **2**, in which *S* is the dNTP, *E* is the polymerase, DNA_n is the substrate oligodeoxynucleotide and DNA_{n+1} is the oligodeoxynucleotide product. The kinetic parameters were determined by fitting the data to equation **2** with the non-linear least squares curve fitting routine in SigmaPlot. Data for Kf(exo$^-$)-catalyzed reactions along with the calculated lines are illustrated in Figure 4. The kinetic parameters are presented in Tables 1–4 and compared in Figure 5.

$$E\text{–DNA}_n + S \leftrightarrows E\text{–DNA}_n\text{–}S \rightarrow E\text{–DNA}_{n+1} \quad \mathbf{1}$$

$$v_o = V_{max}[S]_o/([S]_o + K_m) \quad \mathbf{2}$$

The relative incorporation of dC to dT opposite guanine ranged from 3100 for Tth DNA polymerase to 21 000 for Taq DNA polymerase. The relative V_{max}/K_m for incorporation of dC/dT was 5-fold higher for Kf(exo$^-$) than Kf(exo$^+$). This difference was largely due to a lower K_m for incorporation of dCTP by Kf(exo$^-$). In all cases, preferential incorporation of dC over dT was primarily due to a lower K_m for dCTP. This result is consistent with that previously observed with Kf(exo$^+$) (36).

Table 1. Incorporation of dCTP and dTTP opposite guanine analogs by Klenow (exo$^-$)[a]

Template	dCTP			dTTP		
	V_{max}[b]	K_m[c]	V_{max}/K_m[d]	V_{max}[b]	K_m[c]	V_{max}/K_m[d]
G	22 ± 1	0.014 ± 0.003	1600 ± 320	8.0 ± 0.7	77 ± 22	0.10 ± 0.02
O^{6}mG	31 ± 2	104 ± 14	0.29 ± 0.03	96 ± 2	86 ± 12	1.1 ± 0.1
S^{6}mG	16 ± 1	140 ± 30	0.12 ± 0.02	170 ± 10	190 ± 40	0.89 ± 0.11
O^{6}m1DG	18 ± 2	120 ± 20	0.15 ± 0.02	0.86 ± 0.06	360± 50	0.0024 ± 0.0002
O^{6}mH	8.3 ± 1.1	270 ± 80	0.031 ± 0.005	88 ± 8	110 ± 30	0.84± 0.15

[a]50 mM Tris–HCl, 5 mM $MgCl_2$, 5 mM DTT, 100 μg/ml BSA, 190 nM primer, 210 nM template, 0.45 U/ml Kf(exo$^-$), 37°C. [dNTP] varied from 0 to 500 μM. The errors are standard errors.
[b]nmol/min/U polymerase.
[c]μM.
[d]Per min/(U polymerase/ml).

Table 2. Incorporation of dCTP and dTTP opposite guanine analogs by Klenow (exo$^+$)[a]

Template	dCTP			dTTP		
	V_{max}[b]	K_m[c]	V_{max}/K_m[d]	V_{max}[b]	K_m[c]	V_{max}/K_m[d]
G	28 ± 4	0.042 ± 0.008	670 ± 80	12 ± 1	56 ± 5	0.21 ± 0.01
O^{6}mG	110 ± 20	100 ± 30	1.0 ± 0.2	170 ± 20	97 ± 26	1.8 ± 0.3
S^{6}mG	130 ± 20	230 ± 60	0.57 ± 0.08	140 ± 20	110 ± 20	1.3 ± 0.2
O^{6}m1DG	30 ± 5	280 ± 90	0.10 ± 0.02	1.9 ± 0.2	200± 60	0.010 ± 0.003
O^{6}mH	4.9 ± 0.9	70 ± 50	0.07 ± 0.04	140 ± 10	94 ± 25	1.5 ± 0.3

[a]50 mM Tris–HCl, 5 mM $MgCl_2$, 5 mM DTT, 100 μg/ml BSA, 190 nM primer, 210 nM template, 0.45 U/ml Kf(exo$^-$), 37°C. [dNTP] varied from 0 to 500 μM. The errors are standard errors.
[b]nmol/min/U polymerase.
[c]μM.
[d]Per min/(U polymerase/ml).

Table 3. Incorporation of dCTP and dTTP opposite guanine analogs by Taq DNA polymerase[a]

Template	dCTP			dTTP		
	V_{max}[b]	K_m[c]	V_{max}/K_m[d]	V_{max}[b]	K_m[c]	V_{max}/K_m[d]
G	2.3 ± 0.3	0.99 ± 0.33	2.3 ± 0.6	0.021 ± 0.003	190 ± 60	$(1.1 \pm 0.2) \times 10^{-4}$
O^{6}mG	0.17 ± 0.01	280 ± 30	(6.0± 0.4) x 10^{-4}	0.51 ± 0.05	73 ± 25	$(70 \pm 20) \times 10^{-4}$
S^{6}mG	0.13± 0.02	170 ± 0.02	$(2.0 \pm 0.3) \times 10^{-4}$	0.25 ± 0.02	290 ± 30	$(8.5 \pm 0.5) \times 10^{-4}$
O^{6}m1DG	0.15 ± 0.02	150 ± 50	$(9.8 \pm 2.0) \times 10^{-4}$	0.004 ± 0.001	290± 220	$(0.14 \pm 0.05) \times 10^{-4}$
O^{6}mH	0.011 ± 0.002	110 ± 60	$(0.95 \pm 0.37) \times 10^{-4}$	0.92 ± 0.08	390 ± 50	$(24 \pm 1) \times 10^{-4}$

[a]50 mM Tris–HCl, 5 mM $MgCl_2$, 5 mM DTT, 100 μg/ml BSA, 200 nM primer, 220 nM template, 18.8 U/ml Taq DNA polymerase, 37°C. [dNTP] varied from 0 to 500 μM. The errors are standard errors.
[b]nmol/min/U polymerase.
[c]μM.
[d]Per min/(U polymerase/ml).

Table 4. Incorporation of dCTP and dTTP opposite guanine analogs by Tth DNA polymerase[a]

Template	dCTP			dTTP		
	V_{max}[b]	K_m[c]	V_{max}/K_m[d]	V_{max}[b]	K_m[c]	V_{max}/K_m[d]
G	0.046 ± 0.007	0.022 ± 0.009	2.1± 0.6	0.027± 0.011	380 ± 220	$(0.7 \pm 0.2) \times 10^{-4}$
O^{6}mG	0.18 ± 0.02	290 ± 30	$(6.3\pm 0.3) \times 10^{-4}$	0.53 ± 0.03	86 ± 12	$(36 \pm 4) \times 10^{-4}$
S^{6}mG	0.13 ± 0.02	420 ± 140	$(2.9\pm 0.4) \times 10^{-4}$	0.32 ± 0.030	230 ± 40	$(14\pm 1) \times 10^{-4}$
O^{6}m1DG	0.13 ± 0.01	190 ± 50	$(6.8\pm 1.0) \times 10^{-4}$	0.007 ± 0.002	83± 37	$(0.08 \pm 0.01) \times 10^{-4}$
O^{6}mH	0.026 ± 0.006	460 ± 190	$(0.56\pm 0.09) \times 10^{-4}$	1.0 ± 0.1	310 ± 70	$(33 \pm 4) \times 10^{-4}$

[a]50 mM Tris–HCl, 5 mM $MgCl_2$, 5 mM DTT, 100 μg/ml BSA, 200 nM primer, 220 nM template, 18.8 U/ml Tth DNA polymerase, 37°C. [dNTP] varied from 0 to 500 μM. The errors are standard errors.
[b]nmol/min/U polymerase.
[c]μM.
[d]Per min/(U polymerase/ml).

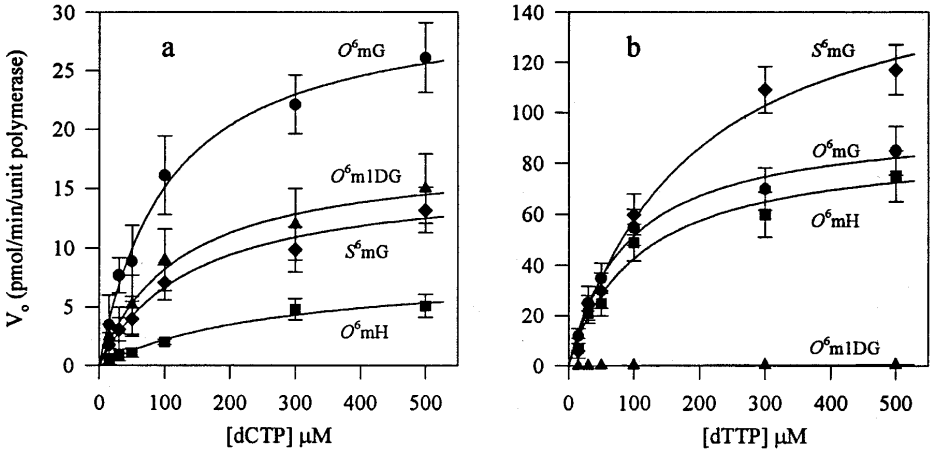

Figure 4. Initial rate of insertion of (**a**) dCTP and (**b**) dTTP opposite templates containing O^6mG (●), O^6m1DG (▲), O^6mH (■) and S^6mG (◆). Each point is an average of three to five determinations and the error bars represent the standard deviations. The lines represent the theoretical hyperbolic curves calculated from the experimental points.

Incorporation of dCTP opposite O^6mG was much slower than opposite G. The difference in V_{max}/K_m was primarily due to an increase in K_m. This result is also consistent with that previously observed with Kf(exo$^+$) (36). Conversely, the V_{max}/K_m for incorporation of dTTP opposite O^6mG was ~10-fold higher than opposite G. This increase was due to a change in the V_{max} for the Klenow fragments and both the V_{max} and K_m parameters for Taq and Tth DNA polymerases.

To determine whether a site on O^6mG is important for incorporation of either dCTP or dTTP, we should examine the change in rate between O^6mG and the analogs in the template. The differences in kinetic parameters are summarized in Figure 5. The largest change in rate was observed in incorporation of dTTP when O^6m1DG replaced O^6mG. The four polymerases exhibited a 500- to 900-fold decrease in V_{max}/K_m, due primarily to a decrease in V_{max}. Substitution of the oxygen with sulfur or removal of the amino group at the 2 position resulted in a <10-fold decrease in V_{max}/K_m in incorporation of dTTP.

The results with O^6m1DG in the template implicate the N1 position of O^6mG as having a critical interaction in incorporation of dTTP. These results are more consistent with the structure in Figure 1b than with that in Figure 1a. If replication occurred via the structure in Figure 1b, then O^6m1DG would be a poor substrate. Replacement of the nitrogen at the 1 position of O^6mG would prevent dTTP from approaching due to steric interactions between the proton at the 1 position of O^6m1DG and the imino proton of dTTP. If, however, replication occurred via the structure in Figure 1a, then we would not predict O^6m1DG to be a poorer substrate then O^6mG, because the orientation of the methoxy group already prevents dTTP from approaching O^6mG and forming an additional hydrogen bond with O^6m1DG.

The model in Figure 1b also predicts a hydrogen bond between the O^2 position of dTTP and the exocyclic amino group of O^6mG. When O^6mG is replaced by O^6mH, this hydrogen bond cannot exist. In contrast to the O^6mG to O^6m1DG substitution, there is no steric interaction which prevents the complexes in Figure 1a or b from forming. This hydrogen bond is important in incorporation of dCTP opposite guanine. Removal of the amino group reduces the rate of reaction ~10-fold (35). Therefore, a decrease in rate would be expected if this interaction is critical. Removal of the amino group from O^6mG, however, did not result in significantly decreased rates of incorporation of dTTP. In contrast to incorporation of dCTP opposite guanine (35), this hydrogen bond is not important in incorporation of dTTP opposite O^6mG.

Table 5. Extension past O^6mG–C and O^6mG–T base pairs[a]

Template	C			T		
	V_{max}[b]	K_m[c]	V_{max}/K_m[d]	V_{max}[b]	K_m[c]	V_{max}/K_m[d]
O^6mG	61 ± 7	58 ± 15	1.05 ± 0.13	65 ± 3	24 ± 3	2.7 ± 0.2
*S*6mG	51 ± 7	49 ± 18	1.06 ± 0.26	82 ± 4	21 ± 3	3.9 ± 0.4
*O*6m1DG	33 ± 2	52 ± 9	0.64 ± 0.08	10 ± 4	54 ± 4	0.19 ± 0.01
*O*6mH	70 ± 6	117 ± 18	0.59 ± 0.05	102 ± 8	24 ± 4	4.2 ± 0.5

[a]50 mM Tris–HCl, 5 mM $MgCl_2$, 5 mM DTT, 100 μg/ml BSA, 190 nM primer, 210 nM template, 0.45 U/ml Kf(exo$^-$), 37°C. [dGTP] varied from 0 to 300 μM. The errors are standard errors.
[b]nmol/min/U polymerase.
[c]μM.
[d]Per min/(U polymerase/ml).

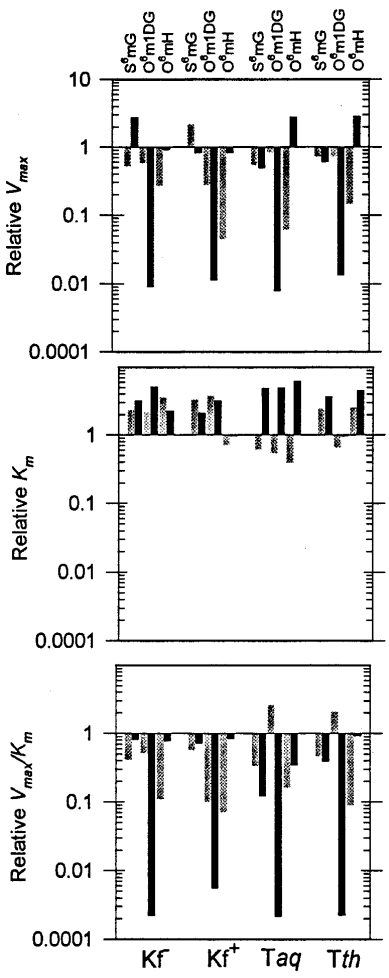

Figure 5. Relative kinetic parameters for insertion of dCTP and dTTP opposite O^6mG, S^6mG, O^6m1DG and O^6mH catalyzed by Kf(exo$^-$), Kf(exo$^+$), Taq and Tth DNA polymerases. The values for the V_{max}, K_m and V_{max}/K_m parameters for insertion of dCTP and dTTP opposite S^6mG, O^6m1DG and O^6mH were divided by the corresponding value for O^6mG.

In insertion of dCTP, alteration of the O^6 and 1 positions of O^6mG produced small changes in the V_{max}/K_m values. Removal of the exocyclic amino group at the 2 position resulted in a larger, ~10-fold, decrease in V_{max}/K_m. These results do not allow us to come to a conclusion as to which structure occurs in the active site of the polymerase during replication.

The small decreases associated with substitution of the O^6 position are consistent with the structures in Figure 2b and c but not a. Substitution of sulfur in the 6 position of guanine has been found to decrease the rate of incorporation of dCTP by 60% (33,34), results similar to those in the present experiments. However, we hesitate to use <10-fold changes in rate to predict structures. S^6mG may subtly differ from O^6mG in properties not associated with binding to dCTP but which may decrease the rate of reaction.

The lack of a large decrease in V_{max}/K_m associated with substitution of the N1 position does not allow us to discriminate between the structures in Figure 2a, b or c. Irrespective of the structure of the O^6mG–dCTP complex, dCTP may be incorporated opposite O^6m1DG by the structure in Figure 2d. Compared with Figure 2c, Figure 2d contains one less hydrogen bond, but is unprotonated. In comparison with Figure 2a and b, Figure 2d has a more Watson–Crick-like geometry, but has one less hydrogen bond. If an analog of O^6mG does not bind to the incoming dNTP as does O^6mG, then analysis of the resulting changes in rate would be very difficult.

The 10-fold decrease in rate observed for substitution of the N^6 position is consistent with the three structures illustrated in Figure 2a–c. The exocyclic amino group of O^6mG has different roles in incorporation of dCTP and dTTP. Removal of this group does not affect the rate of incorporation of dTTP, but reduces the rate of incorporation of dCTP 10-fold. Polymerases have been shown to interact with minor groove sites in the DNA and the incoming dNTP (37–39). Perhaps the minor groove interactions differ depending on whether dCTP or dTTP is incorporated opposite O^6mG.

Extension past O^6mG–C and O^6mG–T base pairs

The extension past O^6mG–C and O^6mG–T base pairs was examined using the template and primer 13C and 13T. The primers were annealed to the four templates and the initial rate of incorporation of dGTP determined. The kinetic analysis was consistent with simple Michaelis–Menten kinetics as illustrated by equations **1** and **2**. The parameters obtained are shown in Table 5. Small changes in rate constants are observed. The largest rate decrease was found in extension past the O^6m1DG–thymine base pair, in a result similar to that found in the insertion reactions. These results are consistent with Figure 1b in extension past O^6mG–dT base pairs.

pH dependency of the incorporation of dCTP and dTTP opposite O^6mG

The possibility of a protonated O^6mG–dCTP complex was tested by examining the pH dependence of incorporation of dCTP and dTTP opposite O^6mG. The O^6mG–dCTP complex can be most Watson–Crick-like when it is protonated (Fig. 2c). In duplex DNA at neutral pH a wobble configuration is more abundant than the protonated species. At more acidic pH the protonated species becomes more abundant (15). If insertion of dCTP opposite O^6mG occurs via the protonated species then the relative rate of incorporation of dCTP should increase at lower pH values. This hypothesis was examined by measuring the relative rates of incorporation of dCTP and dTTP over a pH range.

The competition between incorporation of dCTP and dTTP was measured with both dCTP and dTTP present in the reaction solution. A solution containing 120 μM dCTP and 20 μM dTTP was added to DNA and polymerase. The rates of incorporation of both dCTP and dTTP were at a maximum at pH 8.3 and decreased as the pH was raised or lowered. At pH values <6 the rate of reaction is very slow. These reactions could be detected only with extended incubation times and higher polymerase concentrations. The reaction was quenched and analyzed by PAGE. The products, 13mers containing either C or T on the 3′-end, migrate differently on PAGE and the formation of each was quantified. The relative incorporation divided by the substrate concentrations is equal to the V_{max}/K_m ratios (40) Figure 6 shows $(V_{max}/K_m)^{dCTP}/(V_{max}/K_m)^{dTTP}$ plotted against pH for Kf(exo$^-$), Taq and Tth DNA polymerases.

All of the enzymes exhibit pH-independent $(V_{max}/K_m)^{dCTP}/(V_{max}/K_m)^{dTTP}$ at high pH values. As the pH becomes more acidic, $(V_{max}/K_m)^{dCTP}/(V_{max}/K_m)^{dTTP}$ increases. For Tth DNA polymerases the increase begins below pH 7, for Taq polymerase

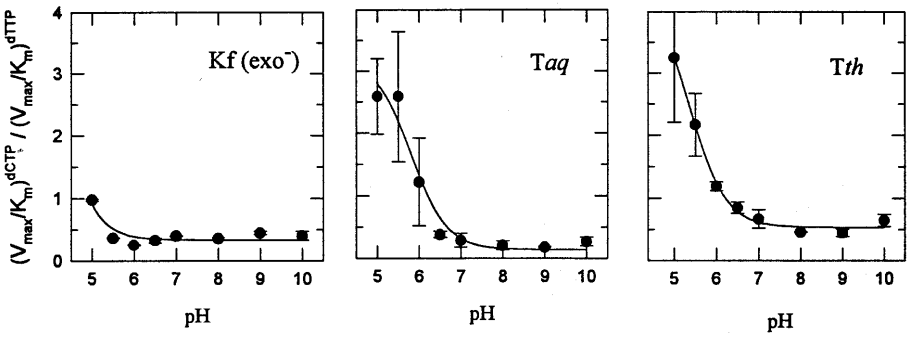

Figure 6. Relative rates of incorporation of dCTP and dTTP opposite O^6mG. The reaction was performed in 50 mM buffer–HCl, 5 mM $MgCl_2$, 5 mM DTT, 100 μg/ml BSA, with an ionic strength of 65 mM containing 20 μM dTTP and 120 μM dCTP. The relative V_{max}/K_m equals (13mer with C/13mer with T)/([dTTP]/[dCTP]). The error bars are the standard deviations. The lines represent the theoretical sigmoid curves calculated from the experimental points.

below pH 6.5 and for Kf(exo⁻) $(V_{max}/K_m)^{dCTP}/(V_{max}/K_m)^{dTTP}$ does not increase until the pH drops below 5.5.

The pH-independent and pH-dependent $(V_{max}/K_m)^{dCTP}/(V_{max}/K_m)^{dTTP}$ regions are consistent with two structures for incorporation of dCTP opposite O^6mG. In the pH-independent regions near physiological pH incorporation of dCTP would occur via a neutral complex such as that in Figure 2a or b. At more acidic pH values dCTP or O^6mG can be protonated and replication can occur via the structure in Figure 2c.

The neutral dCTP–O^6mG structures (Fig. 2a and b) are more distorted from the ideal Watson–Crick geometry than the O^6mG–dTTP complex in Figure 1b. This may contribute to preferential incorporation of dTTP opposite O^6mG. However, at acidic pH values the O^6mG–dCTP complex becomes protonated, adopts a more Watson–Crick-like geometry and dCTP becomes a better substrate than dTTP.

The increase in $(V_{max}/K_m)^{dCTP}/(V_{max}/K_m)^{dTTP}$ occurs at different pH values for each polymerase. The increase for Taq DNA polymerase begins at pH 6.5, at pH 6.0 for Tth DNA polymerase and at pH 5 for Kf(exo⁻). These differences may reflect the relative hydrophobicities of each active site. The more hydrophobic the active site, the lower the pK_a of the dCTP–O^6mG complex would become.

Influence of the 5-methyl group in thymine and cytosine

Neither dCTP nor dTTP is a good substrate for replication opposite O^6mG. Compared with the discrimination between correct and incorrect base pairs, dCTP and dTTP are relatively equal substrates for pairing with O^6mG. The dCTP:dTTP incorporation ratio changes with experimental variables such as nucleotide sequence (41). A difference between cytosine and thymidine is the methyl group at the 5 position of the pyrimidine. The additional hydrophobic surface of the methyl group may enhance stacking ability of the nucleoside onto the primer strand. This factor may make dTTP a better substrate than dCTP for the polymerase. We tested this hypothesis by measuring the relative rates of incorporation of dTTP, dUTP, dCTP and d5mCTP opposite O^6mG.

The initial rates of incorporation of dUTP, dTTP, dCTP and d5mCTP opposite O^6mG catalyzed by Kf(exo⁻) were measured. All four reactions exhibited simple Michaelis–Menten kinetics and the kinetic parameters are shown in Table 6. In incorporation of dTTP removal of the methyl group did not influence rate of reaction. Addition of a methyl group to dCTP increased the rate 2-fold due to a drop in the K_m parameter. Therefore, increased hydrophobicity of the methyl group did not significantly influence whether dCTP or dTTP was incorporated opposite O^6mG.

Table 6. Influence of the 5-methyl group on the insertion of dNTPs opposite O^6mG[a]

dNTP	V_{max}[b]	K_m[c]	V_{max}/K_m[d]
dCTP	34 ± 6	76 ± 17	0.45 ± 0.12
d5mCTP	40 ± 5	45 ± 20	0.89 ± 0.22
dUTP	150 ± 19	88 ± 26	1.7 ± 0.5
dTTP	120 ± 7	71 ± 11	1.7 ± 0.3

[a]50 mM Tris–HCl, 5 mM $MgCl_2$, 5 mM DTT, 100 μg/ml BSA, 190 nM primer, 210 nM template, 0.23 U/ml Kf(exo⁻), 37°C. [dNTP] varied from 0 to 400 μM. The errors are standard errors.
[b]nmol/min/U polymerase.
[c]μM.
[d]Per min/(U polymerase/ml).

CONCLUSION

We have examined the interaction between dCTP and dTTP and O^6mG during DNA replication. The use of analogs of O^6mG have indicated that incorporation of dTTP occurs via the Watson–Crick-like structure indicated in Figure 1b. The pH dependency of incorporation of dCTP/dTTP suggests that dCTP is incorporated opposite O^6mG via an uncharged wobble structure as illustrated in Figure 2a or b. The protonated Watson–Crick-like structure in Figure 2c is a better substrate, but at physiological pH values the O^6mG–dCTP complex is unprotonated.

ACKNOWLEDGEMENTS

This work was funded on NIH grant CA 53625 and a seed grant from cancer center support grant CA 17613.

REFERENCES

1 Loveless,A. (1969) *Nature*, **223**, 206–207.
2 Echols,H. and Goodman,M.F. (1991) *Annu. Rev. Biochem.*, **60**, 477–511.
3 Petruska,J., Goodman,M.F., Boosalis,M.S., Sowers,L.C., Cheong,C. and Tinoco,I.,Jr (1988) *Proc. Natl. Acad. Sci. USA*, **85**, 6252–6256.

4 Petruska,J., Sowers,L.C. and Goodman, M.F. (1986) *Proc. Natl. Acad. Sci. USA*, **83**, 1559–1562.
5 Johnson,K.A. (1993) *Annu. Rev. Biochem.*, **62**, 685–713.
6 Snow,E.T., Foote,R.S. and Mitra,S. (1984) *J. Biol. Chem.*, **259**, 8095–8100.
7 Singer,B., Kusmierik,J.T., Folkman,W., Chavez,F. and Dosanjh,M.K. (1991) *Carcinogenesis*, **12**, 745–747.
8 Loechler,E.L., Green,C.L. and Essigmann,J.M. (1984) *Proc. Natl. Acad. Sci. USA*, **81**, 6271–6275.
9 Chambers,R.W., Sledziewska-Gojska,E. and Hirani-Hojatti,S. (1985) *Proc. Natl. Acad. Sci. USA*, **82**, 7173–7177.
10 Bhanot,O.S. and Ray,A. (1986) *Proc. Natl. Acad. Sci. USA*, **83**, 7348–7352.
11 Hill-Perkins,M., Jones,M.D. and Karran,P. (1986) *Mutat. Res.*, **162**, 153–163.
12 Ellison,K.S., Dogliotti,E., Connors,T.D., Basu,A.K. and Essigmann,J.M. (1989) *Proc. Natl. Acad. Sci. USA*, **86**, 8620–8624.
13 Dosanjh,M.K., Galeros,G., Goodman,M.F. and Singer,B. (1991) *Biochemistry*, **30**, 11595–11599.
14 Tan,H.-B., Swann,P.F. and Chance,E.M. (1994) *Biochemistry*, **33**, 5335–5346.
15 Leonard,G.A., Thomson,J., Watson,W.P. and Brown,T. (1990) *Proc. Natl. Acad. Sci. USA*, **87**, 9573–9676.
16 Gaffney,B.L. and Jones,R.A. (1989) *Biochemistry*, **28**, 5881–5889.
17 Patel,D.J., Shapiro,L., Kozlowski,S.A., Gaffney,B.L. and Jones,R.A. (1986) *Biochemistry*, **25**, 1027–1036.
18 Kalnik,M.W., Li,B.F.L., Swann,P.F. and Patel,D.J. (1989) *Biochemistry*, **28**, 6182–6192.
19 Loechler,E.L. (1991) *Carcinogenesis*, **12**, 1693–1699.
20 Williams,L.D. and Shaw,B.R. (1987) *Proc. Natl. Acad. Sci. USA*, **84**, 1779–1783.
21 Patel,D.J., Shapiro,L., Kozlowski,S.A., Gaffney,B.L. and Jones,R.A. (1986) *Biochemistry*, **25**, 1036–1042.
22 Kalnik,M.W., Li,B.F.L., Swann,P.F. and Patel,D.J. (1989) *Biochemistry*, **28**, 6170–6181.
23 Sriram,M., van der Marel,G.A., Roelen,H.L.P.F., van Boom,J.H. and Wang,A.H.-J. (1992) *Biochemistry*, **31**, 11823–11834.
24 Ginell,S.L., Kuzmich,S., Jones,R.A. and Berman,H.M. (1990) *Biochemistry*, **29**, 10461–10465.
25 Dunn,D.B. and Hall,R.H. (1986) In Fasman,G.D. (ed.), *Handbook of Biochemistry and Molecular Biology*, 3rd Edn. CRC Press, Boca Raton, FL, Vol. 1, pp. 65–215.
26 Spratt,T.E. and de los Santos,H. (1992) *Biochemistry*, **31**, 3688–3694.
27 Spratt,T.E. and Campbell,C.R. (1994) *Biochemistry*, **33**, 11364–11371.
28 Borer,P. (1986) In Fasman,G.D. (ed.), *Handbook of Biochemistry and Molecular Biology*, 3rd Edn. CRC Press, Boca Raton, FL, Vol. 1, p. 589.
29 Strobel,S.A., Cech,T.R., Usman,N. and Beigelman,L. (1994) *Biochemistry*, **33**, 13824–13835.
30 Newman,P.C., Williams,D.M., Cosstick,R., Seela,F. and Connolly,B.A. (1990) *Biochemistry*, **29**, 9902–9910.
31 Waters,T.R. and Connolly,B.A. (1994) *Biochemistry*, **33**, 1812–1819.
32 Frey,M.W., Sowers,L.C., Millar,D.P. and Benkovic,S.J. (1995) *Biochemistry*, **34**, 9185–9192.
33 Rappaport,H.A. (1988) *Nucleic Acids Res.*, **16**, 7253–7267.
34 Rappaport,H.A. (1993) *Biochemistry*, **32**, 3047–3057.
35 Donlin,M.J. and Johnson,K.A. (1994) *Biochemistry*, **33**, 14908–14917.
36 Georgiadis,P., Xu,Y.-Z. and Swann,P.F. (1991) *Biochemistry*, **30**, 11725–11732.
37 Beard,W.A., Osheroff,W.P., Pradad,R., Sawaya,M.R., Jaju,M., Wood,T.G., Kraut,J., Kunkel,T.A. and Wilson,S.H. (1996) *J. Biol. Chem.*, **271**, 12141–12144.
38 Pelletier,H., Sawaya,M.R., Kumar,A., Wilson,S.H. and Kraut,J. (1994) *Science*, **264**, 1891–1903.
39 Kim,Y., Eom,S.H., Wang,J., Lee,D.-S., Suh,S.W. and Steitz,T.A. (1996) *Nature*, **382**, 278–281.
40 Goodman,M.F., Creighton,S., Bloom,L.B. and Petruska,J. (1993) *Crit. Rev. Biochem. Mol. Biol.*, **28**, 83–126.
41 Georgiadis,P., Smith,C.A. and Swann,P.F. (1991) *Cancer Res.*, **51**, 5843–5850.